

New effect in Stark spectroscopy of atomic hydrogen: dynamic resonance

V. P. Gavrilenko and E. A. Oks

All-Union Research Institute of Physicotechnical and Radio-Engineering Measurements
(Submitted 20 May 1980; resubmitted 4 February 1981)
Zh. Eksp. Teor. Fiz. 80, 2150-2162 (June 1981)

We investigate analytically the spectrum of the hydrogen atom in an electric field $E(t) = E_0 \cos \omega t + F$, where $F \perp E_0$. In the case when the splitting in the time-averaged field $\langle E(t) \rangle$ coincides with $(2l-1)\omega$, where $l = 1, 2, 3, \dots$, an effect called dynamic resonance is produced. The resonance occurs between the quasienergy states and is multiparticle and multiphoton. The hydrogen spectral lines undergo additional splitting under these conditions. The theory of dynamic resonance provides a physical explanation of the results of the numerical calculation of the L_α spectrum in crossed electric fields $E_0 \cos \omega t$ and F , as reported by Cohn, Bakshi, and Kalman [Phys. Rev. Lett. 29, 324 (1972)]. We show also that fields with fixed phases and fields with random phases can exert different resonant action on the hydrogen spectral lines that start from levels with $n \geq 3$. The dynamic resonance effect can be experimentally observed and used both in laser physics and in plasma physics (in particular, to detect Langmuir solitons).

PACS numbers: 32.60. + i

§1. INTRODUCTION

Stark splitting of hydrogen line under simultaneous action of a static field F and a dynamic field $E_D(t)$ is of practical interest both for nonlinear optics and for plasma resonance spectroscopy.¹ In a preceding paper³ a similar problem was solved analytically for dynamic fields with random phases

$$E_D(t) = \sum_j E_j \cos(\omega t + \varphi_j).$$

The case considered in Ref. 3 was

$$|F| \gg E_0 = \langle E_D(t) \rangle^2,$$

where the field F determines the quantization of the atom and splits the states with the principal quantum number n into $2n - 1$ sublevels spaced²⁾ $3nF/2 \equiv \omega_F$ apart. At resonance ($\omega \approx \omega_F$) the field $E_D(t)$ splits each Stark sublevel into two quasi-energy states (QES) with quasi-energies

$$\pm \Omega' = \pm [e_\alpha^2 + (\omega - \omega_F)^2]^{1/2}.$$

In particular, if the distribution of the amplitudes of E_j is one-dimensional and $E_j \perp F$, then

$$e_\alpha^2 = \sum_{\alpha' \neq \alpha} |r_{\alpha\alpha'}|^2 E_0^2 / 4. \quad (1)$$

As a result, numerous dips appear on the hydrogen-line profile and their distances from the line center are multiples of $3F/2$. The theory of resonance dips on hydrogen lines was further developed in Refs. 4-6 and found application in the diagnostics of cosmic⁴ and laboratory^{6,7} plasma. We investigate in this paper the splitting of hydrogen lines in a field

$$E(t) = F + E_D(t),$$

where the phase of the dynamic field is fixed 3):

$$E_D(t) = E_0 \cos \omega t.$$

Starting from the results of Ref. 9, one can expect the nonadiabatic effects to be maximal at $F \perp E_0$. We therefore analyze below only the case $F \perp E_0$ (this does not

make the results less general), and observe as a result a new effect called dynamic resonance.

The physical meaning of the effect is explained in §2 and the resonance condition for arbitrary n is derived. In §3 is calculated the resultant splitting of QES with $n = 2$ and the spectrum of the L_α line is obtained. The limits of the validity of the obtained solution are determined in §4. In §5 we explain qualitatively and quantitatively the features of the L_α line spectrum calculation of Kohn, Bakshi, and Kalman (CBK),¹⁰ which remains incomprehensible to this day. In §6 are discussed the results and the prospects of their practical application.

§2. THE GIST OF THE EFFECT

We choose the z axis of the immobile coordinate system along E_0 and the x axis along F . We change over to a rotating frame $x'y'z'$, whose z' axis is directed at each instant of time along the resultant field $E(t)$ and makes an angle $\varphi(t)$ with the z axis (see Fig. 1).

The Hamiltonian of the atom in the $x'y'z'$ system is of the form

$$H = H_0 + V_1(t) + V_2(t), \quad V_1(t) = zE(t), \quad V_2(t) = l_y \dot{\varphi}(t), \quad (2)$$

$$E(t) = |E(t)|, \quad \dot{\varphi}(t) = \omega F E_0 \sin \omega t / E^2(t).$$

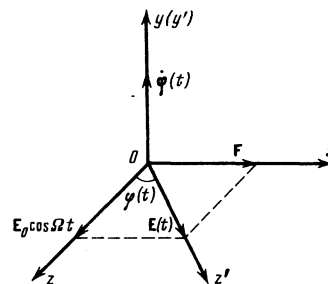


FIG. 1. Geometry of crossed fields. The x axis of the immobile coordinate system xyz is directed along the static field F , and the z axis along the dynamic field $E_0 \cos \omega t$. The coordinate frame $x'y'z'$ rotates with angular velocity $\dot{\varphi}(t)$ relative to the system xyz . The z' axis is directed along the resultant field $E(t)$, and the y and y' axes coincide.

Here H_a is the Hamiltonian of the isolated atom in the xyz system; l_y is the projection of the angular momentum on the y axis. The dc component $V_1(t)$ of the perturbation splits the states with equal n into $2n - 1$ sub-levels with a spacing between them

$$\omega_{\bar{r}} = 3\pi^{-1}n(F^2 + E_0^2)^{1/2}E(k), \quad (3)$$

where $k \equiv E_0(F^2 + E_0^2)^{-1/2}$, and $E(k)$ is a complete elliptic integral of the second kind in its normal form.

If we put $V_2(t) \equiv 0$ in the Hamiltonian (1), then the solutions of the Schrödinger equation can be chosen to be QES with wave functions (WF) $\Psi_\alpha(t)$:

$$\begin{aligned} \Psi_\alpha(t) &= \exp[-i(n_1 - n_2)\omega_{\bar{r}}t] \Phi_\alpha(t), \\ \Phi_\alpha(t) &= \exp\left\{i\left[\omega_{\bar{r}}t^{-3/2}n \int_0^t E(t')\right](n_1 - n_2)\right\} \Psi_\alpha(r) \\ &= \sum_{r=-\infty}^{+\infty} \Phi_{\alpha r}(r) \exp(2is\omega t). \end{aligned}$$

Here $\alpha \equiv (n_1, n_2, m)$ are the parabolic quantum numbers; $\Phi_{\alpha r}(r)$ are Fourier coefficients. We obtain thus QES with the spacing of their quasi-energies equal to

$$Q = \omega_{\bar{r}} + 2u\omega \quad (u=0, \pm 1, \pm 2, \dots).$$

The "magnetic" perturbation $V_2(t)$ has the following Fourier expansion:

$$\begin{aligned} V_2(t) &= l \sum_{v=1}^{\infty} b_v \sin(2v-1)\omega t, \quad b_v = 2(-1)^{v+1} \\ &\times [(1 + F^2 E_0^{-2})^{1/2} - F E_0^{-1}]^{2v-1} \omega. \end{aligned} \quad (4)$$

It is clear that at $Q = (2v - 1)\omega$ multiphoton resonance sets in between many QES harmonics and is due simultaneously to all the harmonics of $V_2(t)$. The possibility of *multifrequency* resonances between QES was indicated by Anosov.¹¹ In our case the resonance condition can be written in the final form

$$\omega_{\bar{r}} = (2l-1)\omega, \quad l=1, 2, 3, \dots \quad (5)$$

The physical meaning of the effect is most evident in the case $E_0 \gg F$, when the dc component of the field is $\bar{E} \equiv \langle |E(t)| \rangle \approx 2E_0/\pi$. Condition (5) means then that an odd harmonic of the dynamic-field frequency coincides with the splitting $\omega_{\bar{r}} \approx (\frac{3}{2})n \cdot 2E_0/\pi$ due essentially to the same *dynamic* field. This is why the effect is called dynamic resonance. We note that although the static field does not enter in the resonance condition at $E_0 \gg F$, it determines the amplitudes b_v of the harmonics of the magnetic perturbation $V_2(t)$ [see Eq. (4)] and the produced QES splitting.

§3. SPECTRUM OF THE L_α LINE IN DYNAMIC RESONANCE

The equations for the matrix elements of the evolution operator take in the interaction representation the form

$$\begin{aligned} i\dot{T}_{\alpha\alpha'} &= \sum_{\alpha''} V_{\alpha\alpha''} T_{\alpha''\alpha'}, \quad V'(t) \\ &= \exp\left[i \int_0^t dt' V_1(t')\right] V_2(t) \exp\left[-i \int_0^t dt' V_1(t')\right]. \end{aligned} \quad (6)$$

Using the resonance approximation, we obtain the solutions of Eqs. (6) for the QES with $n=2$. The stark states from which the matrix elements $T_{\alpha\alpha'}$ are calculated

will be designated in the following manner:

$$(100)=1, \quad (001)=2, \quad (00-1)=3, \quad (010)=4. \quad (7)$$

We expand $E(t)$ in a Fourier series:

$$E(t) = (2l-1)\omega/3 + \sum_{q=1}^{\infty} E_{2q}(l) \cos 2q\omega t.$$

Using (5), we obtain

$$\omega^{-1}E_{2q}(l) = 2(2l-1) [\pi\omega_{\bar{r}}(F, E_0)]^{-1} \int_{-\pi/2}^{\pi/2} dx (F^2 + E_0^2 \cos^2 x)^{1/2} \cos 2qx.$$

The maximum value $|E_{2q}(l)/\omega|_{\max}$ is reached at $F=0$:

$$|\omega^{-1}E_{2q}(l)|_{\max} = 1/3(2l-1) \left| \int_{-\pi/2}^{\pi/2} dx |\cos x| \cos 2qx \right| = 4(2l-1) [3\pi(4q^2-1)]^{-1}. \quad (8)$$

We confine ourselves in (5) to the resonances for $l=1$ and $l=2$. It follows from (8) that

$$1/4 |E_1(1)/\omega|_{\max} = 1/15\pi \ll 1/2 |E_2(1)/\omega|_{\max} = 2/3\pi; \quad (9)$$

$$1/4 |E_2(2)/\omega|_{\max} = 1/5\pi \ll 1/2 |E_1(1)/\omega|_{\max} = 2/3\pi.$$

The inequalities (9) allow us to represent the perturbation, after simple transformations, in the form

$$\begin{aligned} V_{\alpha\alpha'}'(t) &= (l_y)_{\alpha\alpha'} \exp[i(2l-1)(z_{\alpha\alpha} - z_{\alpha'\alpha'})\omega t/3] \\ &\times \left\{ \sum_{u=-\infty}^{+\infty} J_u[(z_{\alpha\alpha} - z_{\alpha'\alpha'})E_0/2\omega] \exp(2iu\omega t) \sum_{v=1}^{\infty} b_v \sin(2v-1)\omega t \right\}. \end{aligned} \quad (10)$$

Since $z_{\alpha\alpha} = 0, \pm 3$, nonoscillating components are contained in (10). We can confine ourselves to them in the calculation of the values of $V_{\alpha\alpha'}'(t)$ in the resonance approximation. In addition, inequalities (9) give grounds for retaining in (10) only the Bessel functions numbered $u=0$ at $l=1$ and $u=0$ and ± 1 at $l=2$. The nonzero matrix elements $V_{\alpha\alpha}'$ are then

$$\begin{aligned} V_{11}' &= V_{21}' = V_{13}' = V_{31}' = V_{12}' = V_{22}' = V_{14}' = V_{34}' = ia(l), \\ ia(1) &= -J_0 b_1/4 \approx -b_1/4, \quad ia(2) = (-J_0 b_2 + J_1 b_1)/4 \approx (3E_2 b_1/4\omega - b_2)/4. \end{aligned}$$

Equations (6) take the form

$$i\dot{T}_{1\alpha''} = T_{1\alpha''} a = (T_{2\alpha''} + T_{3\alpha''}), \quad i\dot{T}_{2\alpha''} = T_{2\alpha''} a = (T_{1\alpha''} + T_{3\alpha''}) \quad (\alpha''=1, 2, 3, 4). \quad (11)$$

Taking the initial conditions $T_{\alpha\alpha'}(0) = \delta_{\alpha\alpha'}$ into account, the system (11) has the following solution:

$$T_{11} = T_{22} = T_{33} = T_{44} = (1 + \cos \Omega t)/2, \quad T_{23} = T_{32} = (\cos \Omega t - 1)/2, \quad (12)$$

$$T_{12} = T_{21} = T_{34} = T_{43} = 1/2 (-1)^{l+1} \sin \Omega t, \quad T_{\alpha\alpha} = T_{\alpha\alpha}.$$

The oscillation frequency $\Omega(l) = 2|a(l)|$ is given by

$$\Omega(1) = b_1/2, \quad \Omega(2) = (3E_2 b_1/4\omega - b_2)/2, \quad (13)$$

$$\begin{aligned} E_2 &= (F^2 + E_0^2)^{1/2} \left\{ \frac{k^2}{4} + \sum_{s=2}^{\infty} \left[\frac{(2s-3)!!}{2^s s!} \right]^2 \frac{(2s-1)2s}{s+1} k^{2s} \right\} \\ &\left(k^2 = \frac{E_0^2}{F^2 + E_0^2} \right). \end{aligned}$$

The spectrum of the L_α line can be represented in the form

$$I(\Delta\omega) = \sum_{l=1}^{\infty} \lim_{T \rightarrow \infty} (2\pi T)^{-1} \left| \int_0^T dt \langle \Psi_l(t) | \mathbf{r} | \Psi_{000} \rangle \exp(-i\Delta\omega t) \right|^2, \quad (14)$$

where $\Delta\omega$ is the distance from the line center

$$\Psi_l(t) = \exp[iu_l \varphi(t)] \exp\left[-iz \int_0^t dt' E(t')\right] T(t) \Psi_l(0)$$

are the WF in the immobile coordinate system [it is as-

which ensures relative smallness of the nonresonant effects.

Thus, for dynamic resonance to exit the static field \mathbf{F} must not be too small $F \gg (E_0)^{1/2}$. This attests once more to the essential role of the static field even if $E_0 \gg F$, when it does not enter in the dynamic-resonance condition (5). It is therefore not surprising that if we put formally $F \rightarrow 0$ in the L_α spectrum at the dynamic resonance (15), this spectrum will not become the known Blokhintsev spectrum¹⁵ whose form for L_α (in the case of transverse observation)

$$I(\Delta\omega) \approx \left[\delta(\Delta\omega) + \sum_{p=-\infty}^{+\infty} J_p^2(3E_0\omega^{-1}) \delta(\Delta\omega - p\omega) \right].$$

At first glance this difference can be due to the use of a rotating frame, in which the quasi-energy spectrum is determined by the expansion of $\exp(3iE_0 \cos \omega t / \omega)$, whereas for the Blokhintsev spectrum we must expand $\exp(3iE_0 \cos \omega t / \omega)$. It is shown in Appendix I.1, however, that the Blokhintsev spectrum (20) can be obtained also if a rotating frame is used (at $F=0$). Thus, the substantial difference between the spectra (15) and (20) is due to another cause, namely, the impossibility in principle of dynamic resonance at $F \ll (\omega E_0)^{1/2}$.

§5. COMPARISON WITH COMPUTER CALCULATION OF THE L_α SPECTRUM

In the CBK paper, the splitting of the L_α line in crossed fields \mathbf{F} and $\mathbf{E}_0 \cos \omega t$ was computer-calculated for eight values of the parameter E_0/ω . It turned out that at certain values of F/ω the E_0/ω structure of the L_α line changes radically: some components vanish and are replaced by others (at new positions). This effect received heretofore no physical explanation.

We change over now to the CBK notation so as to compare their results with those of §3, namely $3F=S$ and $3E_0=D$. In the new notation the resonance condition (5) for $n=2$ becomes

$$D\omega^{-1} = (2l-1)\pi \{2(1+S^2D^{-2})^{1/2} E(k)\}^{-1}, \quad l=1, 2, \dots \quad (k=D(S^2+D^2)^{-1/2}).$$

In the CBK paper the results are represented graphically as plots of k_0/ω vs. S/ω at certain values of D/ω (see Fig. 3, in which the curves of Fig. 1 of the CBK paper are reproduced). The aforementioned radical changes of the L_α spectrum are observed when the function k_0/ω reaches its extrema. According to the CBK definition of the quantity k_0 , it should be connected with the additional splitting by the equation $k_0 = (-1)^l (\Omega - \omega)$.

The comparison with the CBK results was performed in the following manner. Let $D/\omega=0.5$, then the resonance condition (21) at $l=1$ yields $S/D \approx 1.87$; consequently $S/\omega \approx 0.93$. It is seen from Fig. 3 that the value $S/\omega \approx 0.93$ does in fact correspond to an extremum of the function k_0/ω at $D/\omega=0.5$. The splitting frequency calculated from (13) and (4) yields $\Omega/\omega \approx 0.25$ and consequently $k_0/\omega \approx 0.75$, which coincides with the value of k_0/ω at the same extremum in Fig. 4. The theoretical point with coordinates $S/\omega=0.93$, $k_0/\omega=0.75$ is represented by a circle. The other extremum on the $D/\omega=0.5$ curve agrees well with the theoretical point corresponding to $l=2$.

We calculated similarly the theoretical positions of the extrema and the extremal splittings for other values of D/ω . We point out that in the cases $l=1, 3, \dots$ dynamic resonance corresponds to the maxima of the family of functions k_0/ω , and at $l=2, 4, \dots$ to the minima of these functions. It is seen from Fig. 3 that in most cases the theoretical points of the dynamic resonance agree well with the extrema of the numerically calculated curves.⁵⁾

Thus, the previously incomprehensible results of the CBK numerical calculations are accounted for by the dynamic-resonance theory both qualitatively and quantitatively.

Analytic calculations can be performed not only in the dynamic-resonance regions, but also far from them. The L_α spectrum for the case $\omega_F \ll \omega$, calculated analytically in Appendix I.2, explains well the behavior of the curves in Fig. 3 in the region $S/\omega \ll 1$. In particular, it follows from Eq. (A.9) that the slope of the curves⁶⁾ $(\partial k_0/\partial S) - J_0(D/\omega)$ as $S \rightarrow 0$. It is clear therefore that the first maximum of the family of the k_0/ω curves (in the region $S/\omega \leq 1$) vanishes when the parameter D/ω increases to a value $D/\omega = j_{0,1} \approx 2.4$; the first minimum (in the region $S/\omega \leq 3$) vanishes at $D/\omega = j_{0,2} \approx 5.5$, etc. [$j_{0,1}$ and $j_{0,2}$ are zeros of the Bessel function $J_0(D/\omega)$].

For the case $D/\omega \approx 3E_0/\omega \ll 1$, the spectrum of L_α outside the resonances is analytically calculated in Appendix I.3. Formula (A.10) shows, in particular that there is no additional E_0 -dependent shift at all. Comparison of this result with the CBK numerical calculation is, unfortunately, possible only for the k_0/ω curves with the parameters $D/\omega=0$ and $D/\omega=0.5$. The absence of a shift (in the considered approximation) means that the distance between curves should tend to zero off resonance, as is in fact observed.

§6. DISCUSSION OF RESULTS

The dynamic resonance effect observed in the present study via analytic calculation is quite unusual. In this effect, the dynamic field plays alone a double role: it is an external force of definite frequency, and the same time tunes the system frequency proper to resonance. In addition, since the resonant states are not the usual energy states but QES, this resonance has many frequencies: it is produced not by the external force alone, but simultaneously by all its harmonics.

The dynamic-resonance theory provided a physical explanation of the CBK numerical-calculation results. The resonance condition (5), (3) and the dependence (13), (5) of the resonant splitting of Ω on F and E_0 make it possible to choose suitable parameters for setting up an experiment aimed at observing the effect. We note that within the region of validity of the resonance approximation [Eq. (19)] the splitting frequency can reach values $\Omega \approx 0.5\omega$.

The formulas obtained in §§2 and 3 are valid for relatively weak dynamic fields $E_0 \ll F$, when in essence only the fundamental resonance is left ($l=1$). In this case the dynamic resonance has a common physical basis with the results of Ref. 3 for dynamic fields with random

phases. Averaging over the random phases made it possible in Ref. 3 to obtain a general formula for the splittings ε_α at arbitrary n [see Eq. (1)]. Unfortunately, for fields with fixed phase such a calculation is impossible in general form.

The values of ε_α calculated for sublevels with $n=2$ all have equal values $\varepsilon=3E_0/2$, the same as the corresponding splitting $\Omega(1)$ obtained from formulas (13) and (4) for $E_0 \ll F$.

For $n=3$, a detailed spectrum calculation similar to that of §3 is extremely complicated. The splitting frequencies, however, could be obtained. At $l=1$ they take on the values

$$\Omega_2(1) = 2\Omega_1(1) = 2[(1+F^2E_0^{-2})^{1/2} - FE_0^{-1}]\omega. \quad (22)$$

At $E_0 \ll F$ we obtain $\Omega_1(1) = 3E_0/2$ and $\Omega_2(1) = 3E_0$. At the same time, there are three values of ε_α for $n=3$ ($\varepsilon_1 = 9\sqrt{2}E_0/4 \approx 3.18E_0$, $\varepsilon_2 = 9\sqrt{3}E_0/4 \approx 3.90E_0$, and $\varepsilon_3 = 9E_0/2$), none of which agree with $\Omega_1(1)$ or $\Omega_2(1)$.

Consequently, resonant action of fields with random phases and of fields with fixed phase yield the same result only for the L_α line, while for the other hydrogen lines the resonance splitting depends on the character of the phase shifts. In other words, by using hydrogen spectral lines starting with levels $n \geq 3$ one can directly distinguish fields with random phases from those with fixed phase, even if their other parameters (ω, E_0) coincide. This result is of interest not only theoretically, but also from the practical point of view: it can serve, for example, as a basis for a procedure for the diagnostics of Langmuir solitons, capable of distinguishing them from oscillations with random phases.

The dynamic-resonance effect can thus be experimentally observed and used both in laser physics and in plasma physics.

APPENDIX I

L_α spectra off resonance

1.1. OBTAINING THE BLOKHINTSEV L_α SPECTRUM USING A ROTATING COORDINATE FRAME

In the case $F=0$ the Schrödinger equation in the rotating frame is of the form

$$i\partial\Psi/\partial t = [zE_0|\cos\omega t| + l_\varphi\dot{\varphi}(t)]\Psi; \quad (A.1)$$

$$\varphi(t) = 0 \quad (\max(4j-5, 0) < 2\pi^{-1}\omega t < 4j-3);$$

$$\varphi(t) = \pi \quad (4j-3 < 2\pi^{-1}\omega t < 4j-1); \quad j=1, 2, \dots$$

Assume that at $0 \leq t \leq \pi/2\omega$ the atom in the rotating frame was described by the WF $\Psi_{\text{rot}} = \Psi_{100}(\mathbf{r}) \times \exp[-(3iE_0/\omega)\sin\omega t]$. At the instant $t = \pi/2\omega$ the quantization direction is instantaneously reversed. In this case, in view of the suddenness of the perturbation $l_\varphi\dot{\varphi}(t)$ there is no time for anything to happen to the atom—its state (100) is only renamed (010) and remains the same up to the instant $3\pi/2\omega$, when it is again renamed (100), and so forth. We therefore seek the solution in the form

$$\Psi_{\text{rot}} = \left[\sum_{i=1}^4 \alpha_i(\varphi) \Psi_i(\mathbf{r}) \right] \exp(-3iE_0\omega^{-1}\sin\omega t), \quad (A.2)$$

in which the coefficients α_i depend on the time via the discontinuous function $\varphi(t)$ [the four states with $n=2$ are numbered here in accord with Eq. (7)]. Substituting (A.2) in (A.1) and using the matrix elements $(l_\varphi)_{i'i}$ calculated from the formulas of Appendix II, we get

$$\dot{\alpha}_{1,4} = \mp 3iE_0(|\cos\omega t| \mp \cos\omega t) \alpha_{1,4} \pm 1/2\dot{\varphi}(\alpha_2 + \alpha_3), \quad (A.3)$$

$$\dot{\alpha}_{2,3} = 1/2\dot{\varphi}(-\alpha_1 + \alpha_4) + (3iE_0 \cos\omega t) \alpha_{2,3}.$$

We seek a solution of (A.3) in the form

$$\alpha_i = A_i + B_i \cos\varphi(t) + C_i \sin\varphi(t).$$

We use here important identities that play the central role the present section:

$$\cos\omega t \sin\varphi(t) = 0, \quad \cos\omega t \cos\varphi(t) = |\cos\omega t|, \quad |\cos\omega t| \cos\varphi(t) = \cos\omega t.$$

In the upshot we get

$$\alpha_{1,4} = 1/2[1 \pm \cos\varphi(t)], \quad \alpha_{2,3} = \alpha_3 = -1/2 \sin\varphi(t), \quad (A.4)$$

thereby determining the WF in the rotating coordinate system.

The WF Ψ_{rest} in the immobile coordinate system is

$$\Psi_{\text{rest}} = \exp[i l_\varphi \varphi(t)] \Psi_{\text{rot}}. \quad (A.5)$$

In what follows we need the relations

$$2 \exp(i l_\varphi \varphi) |1\rangle = (1 + \cos\varphi) |1\rangle + \sin\varphi (|2\rangle + |3\rangle) + (1 - \cos\varphi) |4\rangle,$$

$$2 \exp(i l_\varphi \varphi) |2\rangle = -\sin\varphi (|1\rangle - |4\rangle) + (1 + \cos\varphi) |2\rangle - (1 - \cos\varphi) |3\rangle, \quad (A.6)$$

$$2 \exp(i l_\varphi \varphi) |3\rangle = -\sin\varphi (|1\rangle - |4\rangle) - (1 - \cos\varphi) |2\rangle + (1 + \cos\varphi) |3\rangle,$$

$$2 \exp(i l_\varphi \varphi) |4\rangle = (1 - \cos\varphi) |1\rangle - \sin\varphi (|2\rangle + |3\rangle) + (1 + \cos\varphi) |4\rangle.$$

Substituting (A.2) in (A.6) and taking (A.4) and (A.6) into account, we obtain ultimately

$$\Psi_{\text{rest}} = \Psi_i(\mathbf{r}) \exp(-3iE_0\omega^{-1}\sin\omega t),$$

which agrees with Blokhintsev's results.¹⁵ The L_α spectrum is determined by formula (20) (when observed in a direction perpendicular to E_0).

1.2. L_α SPECTRUM IN THE CASE $3F \equiv \omega_F \ll \omega$

In the crossed fields F and $E_0 \cos\omega t$, the Schrödinger equation in the immobile coordinate system is of the form

$$i\partial\Psi/\partial t = (H_0 + zE_0 \cos\omega t + zF)\Psi. \quad (A.7)$$

We seek the WF in the form

$$\Psi(t) = \sum_{i=1}^4 C_i(t) \Psi_i(t),$$

where $\Psi_i(t)$ is the WF which is the solution of Eq. (A.7) at $F=0$:

$$\Psi_{1,4}(t) = \Psi_{1,4}(\mathbf{r}) \exp(\mp i\chi \sin\omega t), \quad \Psi_{2,3}(t) = \Psi_{2,3}(\mathbf{r}), \quad \chi = 3E_0\omega^{-1},$$

[the numbering of the states with $n=0$ corresponds to Eq. (7)]. For the coefficients $C_i(t)$ we have

$$C_1 = -1/2 i\omega_F (C_2 + C_3) \exp(i\chi \sin\omega t) = C_1 \exp(2i\chi \sin\omega t), \quad (A.8)$$

$$C_2 = C_3 = -1/2 i\omega_F [C_1 \exp(-i\chi \sin\omega t) + C_4 \exp(i\chi \sin\omega t)].$$

The solution of the system (A.8) depends on the initial conditions. In particular, for $C_i(0) = \delta_{i1}$ we can obtain

$$C_{1,4}(t) = \{\pm 1 + \cos[\omega_F J_0(\chi)t] + f_{1,4}(\chi, t)\}/2,$$

$$C_2(t) = C_3(t) = -i \{ \sin[\omega_F J_0(\chi)t] + f_2(\chi, t) \}/2.$$

Here $f_i(\chi, 0) = 0$ and $\lim_{t \rightarrow 0} f_i(\chi, t) = 0$ as $(\omega_F/\omega) \rightarrow 0$, $i=1, 2, 3, 4$. The obtained solutions of the system (A.8) enable us

to obtain the following spectrum of L_α (for observation transverse to \mathbf{F} and \mathbf{E}_0):

$$I(\Delta\omega) \propto \left\{ [\delta(\Delta\omega - \omega_p J_0(\chi)) + \delta(\Delta\omega + \omega_p J_0(\chi))] / 2 + \sum_{p=-\infty}^{+\infty} \{ J_{2p}^2(\chi) \delta(\Delta\omega - 2p\omega) + J_{2p+1}^2(\chi) [\delta(\Delta\omega - (2p+1)\omega - \omega_p J_0(\chi)) + \delta(\Delta\omega - (2p+1)\omega + \omega_p J_0(\chi))] / 2 \} \right\}. \quad (\text{A.9})$$

It follows from (A.9) that at $\omega_p = 0$ the spectrum $I(\Delta\omega)$ goes over into the Blokhintsev spectrum (20), and when ω_p increases the even satellites of the lateral component do not split, while the odd ones split into two symmetrical sublines with half the intensity. In particular, at $\chi = 1.5$ formula (A.9) describes well the region $S/\omega \ll 1$ of the L_α spectrum shown in Fig. 2 of the CBK paper.

1.3. L_α SPECTRUM IN THE CASE $3E_0/\omega \equiv \chi \ll 1$

In this case the system (A.8) can be solved analytically, using only the first two terms of the expansion of $\exp(\pm i\chi \sin\omega t)$ in powers of χ . As a result we obtain the following L_α spectrum (observed perpendicular to \mathbf{F} and \mathbf{E}_0):

$$I(\Delta\omega) \propto \left\{ [1 - 1/2\chi^2\omega^2(\omega^2 + 2\omega_p^2)(\omega^2 - \omega_p^2)^{-2}] \delta(\Delta\omega) + 1/2[\delta(\Delta\omega - \omega_p) + \delta(\Delta\omega + \omega_p)] + 1/8\chi^2\omega^2\{(\omega + \omega_p)^{-2} \times [\delta(\Delta\omega - (\omega + \omega_p)) + \delta(\Delta\omega + (\omega + \omega_p))] + (\omega - \omega_p)^{-2} \times [\delta(\Delta\omega - (\omega - \omega_p)) + \delta(\Delta\omega + (\omega - \omega_p))] + 2\omega_p^2(\omega^2 - \omega_p^2)^{-2} \times [\delta(\Delta\omega - \omega) + \delta(\Delta\omega + \omega)]\} \right\}. \quad (\text{A.10})$$

We recall that Eq. (A.10) does not hold near the resonances (5), the condition for which at $\chi \ll 1$ is of the form $\omega_p \approx (2l - 1)\omega$.

APPENDIX II

THE MATRIX ELEMENTS $(l_-)_{\alpha'\alpha}$

In the present paper we use matrix elements $(l_y)_{\alpha'\alpha}$ determined from the WF in parabolic coordinates. They can be obtained by starting from the values of the matrix elements $(l_-)_{\alpha'\alpha}$. The latter were calculated in Ref. 14 for the case of a magnetic quantum number $m \geq 1$:

$$\langle n_1' n_2' m - 1 | l_- | n_1 n_2 m \rangle = \begin{cases} -[(n_2 + 1)(n - n_2 - 1)]^{1/2}, & n_1' = n_1, \quad n_2' = n_2 + 1 \\ [(n_1 + 1)(n - n_1 - 1)]^{1/2}, & n_1' = n_1 + 1, \quad n_2' = n_2 \end{cases}$$

We present the values of the matrix elements $(l_-)_{\alpha'\alpha}$ at $m \leq 0$:

$$\langle n_1' n_2' m - 1 | l_- | n_1 n_2 m \rangle = \begin{cases} [n_2(n - n_2)]^{1/2}, & n_1' = n_1, \quad n_2' = n_2 - 1 \\ -[n_1(n - n_1)]^{1/2}, & n_1' = n_1 - 1, \quad n_2' = n_2 \end{cases}$$

¹⁾ Plasma resonance spectroscopy is defined here as investigation of the effects produced in the optical line spectrum of a plasma by lifting the degeneracy of the atom + field system as a result of their interaction. The first pertinent experiments¹⁻³ have shown that, relaxation processes not-

withstanding, the evolution of a two- or multilevel atom in a plasma can have a dynamic character under conditions of resonance with a (quasi)monochromatic field.

- ²⁾ Here and elsewhere we use the atomic units $\hbar = m = e = 1$.
³⁾ A field of this type is produced, for example, when a plasma is acted upon by laser radiation (of frequency $\omega > \omega_{pe}$) or if strong Langmuir turbulence (solitons⁶) with a quasi-one-dimensional spectrum is produced in plasma. The static component of \mathbf{F} is due to the low-frequency electrostatic oscillations and (or) ion microfields.
⁴⁾ Strictly speaking, for formula (17) to be correct it is necessary to satisfy also the condition $\omega_p \gg \omega$, under which the integrals over the segments $(j-1)\pi/\omega \leq t \leq j\pi/\omega$ can be replaced by integrals such as (16) with infinite limits. We point out also that at $y \sim \eta^{-1} \gg 1$ we can put $K_{1/3}(y) \approx (\pi/2y)^{1/2} e^{-y}$.
⁵⁾ At $D/\omega = 1.5$ the minimum of k_0/ω indicated by CBK in their Fig. 1 does not correspond to the splitting shown by them in Fig. 2 of Ref. 10 for the same $D/\omega = 1.5$. Since the value of k_0/ω for $D/\omega = 1.5$ in Fig. 1 of Ref. 10 does not correspond to the smooth variation of the minima of the functions k_0/ω for different D/ω , it appears that at $D/\omega = 1.5$ the correct values of k_0/ω are those corresponding to Fig. 2 of Ref. 10. They are shown dashed in our Fig. 3. For the minimum of k_0/ω at $D/\omega = 1$ the situation is similar. Since the condition, expressed by (19), for the validity of theory is not fulfilled, the theoretical points are not marked on the curves with $D/\omega = 1.5$ and $D/\omega = 2$ in the case $l = 1$, nor on the curve with $D/\omega = 4.5$ in the case $l = 2$.

⁶⁾ This circumstance was noted by CBK.

¹D. Prosnitz and E. V. George, Phys. Rev. Lett. **32**, 1282 (1974).

²D. Prosnitz, D. W. Wildman, and E. V. George, Phys. Rev. **A13**, 891 (1976).

³E. A. Oks, Pis'ma Astr. Zh. **4**, 415 (1978) [Sov. Astron. Lett. **4**, 223 (1978)].

⁴A. I. Zhuzhunashvili and E. A. Oks, Zh. Eksp. Teor. Fiz. **73**, 2142 (1977) [Sov. Phys. JETP **46**, 1122 (1977)].

⁵E. A. Oks, in: Issledovaniya v oblasti radiotekhnicheskikh izmerenii (Radio-Measurement Research), VNIIFTRI (Res. Inst. for Physicotech. and Radio Eng. Measurements), No. 40(70), 89 (1979).

⁶E. A. Oks and V. A. Rantsev-Kartinov, Zh. Eksp. Teor. Fiz. **79**, 99 (1980) [Sov. Phys. JETP **52**, 58 (1980)].

⁷K. H. Finken, R. Buchwald, G. Bertchinger, and H.-J. Kunze, Phys. Rev. **A21**, 200 (1980).

⁸B. B. Kadomtsev, Kollektivnye yavleniya v plazme (Collective Phenomena in Plasma), Nauka, 1976, Chaps. 3 and 5.

⁹E. A. Oks and G. V. Sholin, Opt. Spekt. **42**, 761 (1977) [Opt. Spectrosc. **42**, 434 (1977)].

¹⁰A. Cohn, P. Bakshi, and G. Kalman, Phys. Rev. Lett. **29**, 324 (1972).

¹¹M. D. Ansonov, Opt. Spektrosk. **47**, 209 (1979) [Opt. Spectrosc. **47**, 121 (1979)].

¹²J. I. Rabi, Phys. Rev. **15**, 652 (1937).

¹³A. Messiah, Quantum Mechanics, New Holland, 1965, Vol. 2 Chap. 17, §13.

¹⁴G. V. Sholin, A. V. Demura, and V. S. Lisitsa, Zh. Eksp. Teor. Fiz. **64**, 2097 (1973) [Sov. Phys. JETP **37**, 1057 (1973)].

¹⁵D. I. Blochintzev, Phys. Zs. Sow. Union **4**, 501 (1933).

Translated by J. G. Adashko